A comparative study of photocatalytic degradation of 3-chloropyridine under UV and solar light by homogeneous (photo-Fenton) and heterogeneous (TiO₂) photocatalysis

M.C. Ortega-Liébana, E. Sánchez-López, J. Hidalgo-Carrillo, A. Marinas *, J.M. Marinas, F.J. Urbano

Organic Chemistry Department, University of Córdoba, Campus de Excelencia Agroalimentario, ceiA3, Marie Curie Building E-14014, Córdoba, Spain

ARTICLE INFO

ABSTRACT

Photocatalytic degradation of 3-chloropyridine in the homogeneous (photo-Fenton) and heterogeneous (TiO₂) phase was studied using both UV and sun light. Complete mineralization was achieved in both cases though times required in photo-Fenton process were ca. 5 times shorter under our experimental conditions. Results found at lab scale (solar simulator) were successfully extrapolated to a larger scale (30 L) thus evidencing the validity of the method for treatment of waters polluted with this kind of chemical. Toxicity tests (*Vibrio fischeri*) showed that some intermediates more toxic than 3-chloropyridine were formed as reaction proceeded.
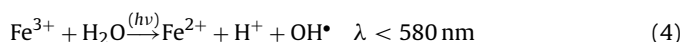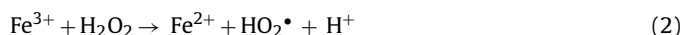
1. Introduction

Pesticides are considered important surface and ground water contaminants [1]. These contaminants are introduced into the environmental system through crops disinfection, industrial pesticide cleaning, misuse and lack of understanding of their ecological effects. The biological treatment is considered the typical process for natural decontamination. Unfortunately, all organic pollutants are not biodegradable and there is a class of products noted as bio-recalcitrant organic compounds.

Consequently, the development of new eco-friendly methods for destroying these pollutants has become an imperative task, advanced oxidation processes (AOPs) being an interesting choice [2]. AOPs rely on in situ generation of highly reactive radical species, OH• mainly, by using solar, chemical or other forms of energy [3]. The most attractive feature of AOPs is that these highly oxidant radicals allow the non-selective destruction of a wide range of organic chemicals. Therefore, AOPs consist in the addition or generation of highly oxidizing species to achieve the mineralization of organic matter [2,4,5]. Frequently, they are employed to degrade toxic pollutants as a previous step, coupled to a subsequent biological treatment [6–8].

Among the AOPs, solar photocatalysis [9] involves the use of solar light as energy source to generate hydroxyl radicals. In this case, a catalyst is needed to absorb the solar light (visible and/or near UV radiation). The most widely used photocatalysts are titanium dioxide, photo-Fenton catalyst and solar sensitisers [10]. In the present study, the two first options are used.

Fenton process involves the use of Fe^{2+} and H_2O_2 thus resulting in the production of 1 hydroxyl radical per molecule of hydrogen peroxide (Eq. (1)). In excess of H_2O_2, two ferrous irons can be regenerated at the expense of one H_2O_2 molecule (Eqs. (2) and (3)). If Fenton process is conducted in the presence of UV–Vis light (photo-Fenton process), Fe(II) species can be regenerated through equation 4 and iron (II) can be considered as true catalytic species.

$$Fe^{2+} + H_2O_2 \rightarrow Fe^{3+} + OH^- + OH^• \tag{1}$$

$$Fe^{3+} + H_2O_2 \rightarrow Fe^{2+} + HO_2^• + H^+ \tag{2}$$

$$Fe^{3+} + HO_2^• \rightarrow Fe^{2+} + O_2 + H^+ \tag{3}$$

$$Fe^{3+} + H_2O \overset{(h\nu)}{\longrightarrow} Fe^{2+} + H^+ + OH^• \quad \lambda < 580\,nm \tag{4}$$

In the case of TiO₂ photocatalysis, reactions involved are as follows:

$$TiO_2 + h\nu \rightarrow h^+ + e^- \quad \lambda < 400\,nm \tag{5}$$
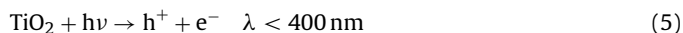
(formation of holes and electrons in valence and conduction band, respectively)

Hydroxyl radicals can be formed through:

$$h^+ + H_2O \rightarrow OH^• + H^+ \tag{6}$$

$$h^+ + OH^- \rightarrow OH^• \tag{7}$$

* Corresponding author. Tel.: +34 957218622; fax: +34 957212066.
 E-mail address: alberto.marinas@uco.es (A. Marinas).

Some previous studies have focused on TiO_2-mediated photocatalytic degradation of chloropyridines using UV light as these compounds are important intermediates in organic synthesis in pharmaceutical industry (antirythmic or antihistaminic compounds) as well as agrochemistry (fungicides and pyridine herbicides) [11–16]. In heterogeneous photocatalysis studies (TiO_2), our research group found that 3-chloropyridine and 2-chloropyridine disappearance follow a zero-order and a first-order kinetics, respectively, and that 2-chloropyridine exhibits stronger adsorption in competitive experiments. As for the reaction mechanisms, SPME–GC–MS studies allowed us to detect some reaction intermediates and propose two parallel degradation routes with hydroxylation and ring opening prior to or after the release of chloride ions. Complete mineralization was achieved under our experimental conditions [14].

The present study represents a step forward comparing homogeneous (photo-Fenton) and heterogeneous (TiO_2) photocatalytic degradation of 3-chloropyridine under both UV and sun light and considering scaling-up of solar photo-Fenton process. Given the rapid disappearance of the substrate, thus resulting in no UV signals within a few minutes of irradiation, total organic carbon evolution (which inform on complete mineralization) is used as the main criterion of comparison. Moreover, toxicity studies are performed by *Vibrio fischeri* assay in order to monitor the potential formation of reaction intermediates or products more toxic than the main substrate itself (3-chloropyridine).

This work must be seen in the context of a project on sustainability of olive oil production carried out in our department and supported by Junta de Andalucía. This project involves the development of a solar-driven photocatalytic method to destroy pesticide residues present in waters coming from olives washing during olive oil production. 3-Chloropyridine was chosen as a model compound of some pyridine pesticides typically used in olive trees (e.g. fluroxypyr).

2. Experimental

2.1. Chemicals

Photocatalytic experiments were carried out using 40 ppm water solutions of 3-chloropyridine (99%, re. C70002 from Sigma–Aldrich). Photo-Fenton experiments were performed using iron sulfate ($FeSO_4 \cdot 7H_2O$, 215422, $\geq$99%, ACS reagent) or chloride ($FeCl_2 \cdot 4H_2O$, 220299, ReagentPlus® 98%), hydrogen peroxide (30%, w/v, re. 95321) (all of them from Sigma–Aldrich) and sulfuric (95–98%, 141058) or hydrochloric acid (37%, re. 141020) (depending on the iron precursor, both from Panreac) for pH 2.8 adjustment. For experiments in the presence of phosphate ions, $Na_3PO_4 \cdot H_2O$ (95%, Panreac re. 141681) was used. Prior to analyses, photo-Fenton treated solutions were neutralized using reagent-grade NaOH (Panreac, re. 141687). A Hanna-Instruments kit (re. 3844) was used for H_2O_2 iodometric determination. Chemicals used for *V. fischeri* bioassay determination include 2% sodium chloride solution and marine bacterium *V. fisheri* (NRRL number B-111777) provided by Macherey-Nagel whereas bovine liver catalase (Sigma–Aldrich, C1345) was used for H_2O_2 elimination.

For heterogeneous photocatalysis experiments, Degussa P25 titanium dioxide (surface area 55 $m^2 g^{-1}$) was used.

2.2. Analytical determinations

Prior to analyses, samples from photo-Fenton studies were neutralized (pH 7) with 0.5 M NaOH to precipitate iron. They were then centrifuged and filtered (0.2 μm Millex nylon membrane filters from Millipore). In the case of heterogeneous photocatalysis (TiO_2), no pH adjustment was necessary prior to centrifugation and filtration.

Mineralization was monitored by measuring the total organic carbon (TOC) with a Shimadzu TOC-V_{CSN} analyzer which was calibrated with standard solutions of potassium phthalate.

Hydrogen peroxide was analyzed by iodometric titration. Therefore, it involved the reaction of hydrogen peroxide with iodide in acid solution followed by titration of liberated iodine with a standard solution of sodium thiosulfate (using a starch indicator).

A commercial bioassay marketed as Biofix® Lumi-10 (Macherey-Nagel) was used for toxicity evaluation of samples partially oxidized by photo-Fenton. Preparation of samples consisted in: (i) elimination of hydrogen peroxide present in the samples from photo-Fenton experiments using bovine liver catalase (ii) filtration (0.2 μm Millex nylon membrane filters from Millipore) and (iii) salinity adjustment to 2% with a NaCl solution. The reagent was a freeze-dried preparation of a specially selected strain of the marine bacterium *V. fischeri* which after 30 min in the fridge at 4 °C was reconstituted with a salty solution. 4 mL of reconstituted bacteria was placed in an incubation block (LUMIStherm from Dr Lange) at 15 °C and luminescence was measured after 10 min. 500 μL of reconstituted bacteria were then added to 500 μL sample from photo-Fenton experiments kept in the incubation block and sample inhibition effect on bacteria was analyzed by measuring the drop in light emission after contact periods of 15 min and comparing it with a toxicant-free control sample (2% sodium chloride solution).

2.3. Photocatalytic experiments

2.3.1. Small-scale photochemical reactions using UV or solar light

Lab-scale experiments were performed on a 20 mL glass heart-shaped three-necked reactor open to the air (Fig. 1A). Solution (suspension in the case of TiO_2) was continuously agitated (900 rpm). Temperature was kept at 25 °C using a water cooling jacket. Radiation was focused on the reactor through an optical fiber. In the case of operating with UV light, a UV Spotlight source Lightningcure™ L8022 from Hamamatsu, with a maximum emission at 365 nm, was used. For sunlight experiments, a solar simulator consisting of a 150 W Xe lamp, ozone free (Newport Re. 6255) was utilized. Lamp outputs as measured at 365 nm were 360 mW cm^{-2} and 618 mW cm^{-2} for solar simulator and UV lamp, respectively. Further details on the spectral distribution of lamps, as provided by the suppliers [17,18], are given in Fig. 2.

2.3.2. Photochemical reactions in the solar-CPC unit

Large-scale solar photochemical experiments were performed in a pilot plant purchased from Ecosystem SA (Barcelona, Spain), Fig. 1B. It consists in a compound parabolic collector (CPC) solar photoreactor (re. Solardetox® Acadus-2008/2.0) with 16 borosilicate tubes and aluminium reflectors tilted 45°. Total collector surface is 2 m^2 and illuminated volume is 15.1 L (30 L being the total volume pumped at 2.1 $m^3 h^{-1}$ from a reservoir). The plant is also equipped with temperature, dissolved oxygen and UV-radiation (ACADUD 85-PLS radiometer) sensors whose data are sent to a computer.

Under standard conditions, 20 mL (lab scale) or 30 L (pilot plant) of a 40 ppm aqueous solution of 3-chloropyridine was irradiated. For photo-Fenton studies 0.88 mM $FeSO_4 \cdot 7H_2O$ (or $FeCl_2 \cdot 4H_2O$ when the effect of chloride ions was studied) was used, with $[H_2O_2]/[3\text{-chloropyridine}] = 25$ and $[H_2O_2]/[Fe^{2+}] = 10$. Initial pH was adjusted to 2.8 (in order to prevent iron salt precipitation) with H_2SO_4 0.5 M or HCl 0.5 M (depending on the iron precursor being sulfate or chloride, respectively) and no extra H_2O_2 was supplied as the reaction proceeded. In the case of heterogeneous photocatalysis experiments, a slurry suspension (700 mg/L) of Degussa P25 was
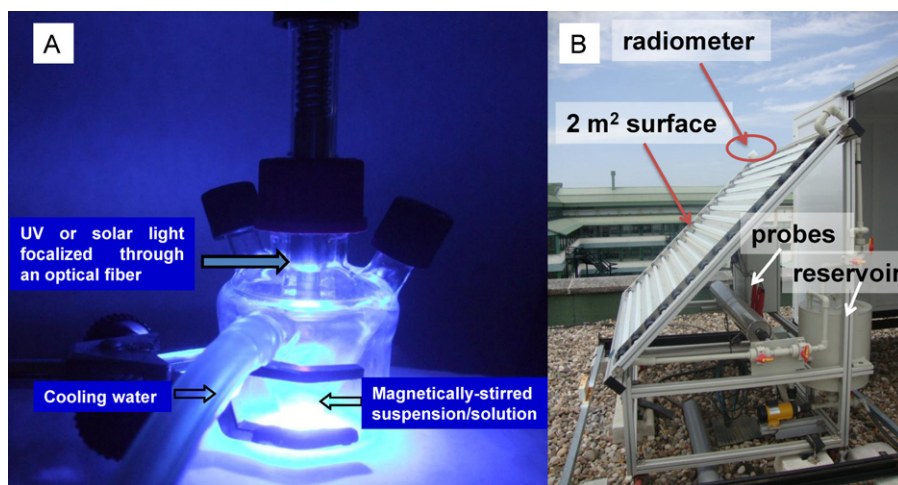
Fig. 1. (A) Experimental device used for lab-scale experiments with light focalized through an optical fiber (reactor volume 20 mL). (B) Larger scale solar photoreactor (irradiated volume 15.1 L, 30 L in total recirculated using a pump).

used (i.e. 10-fold the amount of Fe(II) in photo-Fenton process) and reactions were conducted under natural pH (ca. 6.8). Reactors were opened to the air and no extra oxygen/air was supplied through sparging.

3. Results and discussion

3.1. Fenton, photo-Fenton and direct photolysis

Preliminary results found at lab scale (20 mL reactor) using the solar simulator are summarized in Fig. 3. From that figure, it is evident that even though Fe (II) ions facilitate mineralization of 3-chloropyridine in the presence of H_2O_2 (see Eqs. (1)–(3) in Section 1) the process is much faster in the presence of light (photo-Fenton), as a result of the theoretical generation of 2 $OH^\bullet$ species per molecule of H_2O_2 (see Eqs. (1) and (4)). Therefore, 100% mineralization is achieved through photo-Fenton process after 120 min of irradiation whereas after 170 min only 22% of mineralization is achieved by the Fenton-process despite the almost complete disappearance of H_2O_2 (Fig. 2B). In fact, in the absence of light, regeneration of Fe^{2+} species occurs at the expense of H_2O_2 through Eqs. (2) and (3). From Fig. 3A it is also clear that under our experimental conditions there is no mineralization through direct photolysis whereas when the solution is irradiated in absence of

iron but in the presence of H_2O_2 mineralization occurs to a certain extent (7% after 170 min of irradiation), as a result of generation of hydroxyl radicals via Eq. (8).

$$H_2O_2 + h\nu \rightarrow 2OH^\bullet \quad \lambda < 310\,nm \tag{8}$$
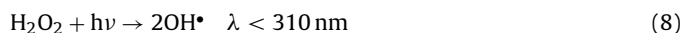
Since this reaction requires energy below 310 nm, only a minor part of solar simulator irradiation is used which accounts for the low percentage of mineralization and, consequently, the fact that 74% of initial H_2O_2 remains after 170 min of irradiation (Fig. 3B).

3.2. Photo-Fenton vs. TiO_2 photocatalysis

Fig. 4 summarizes some results found for photo-Fenton and TiO_2 photocatalysis using the lab-scale reactor and both UV and sun light (solar simulator). It is important to note that TOC abatement was faster for photo-Fenton experiments as compared to TiO_2 photocatalysis both under UV and solar irradiation, even though a molar concentration 10 times higher for TiO_2 as compared to Fe^{2+} was utilized. This suggests a better use of light in photo-Fenton process. Therefore, for instance, time required for 100% mineralization using UV light was ca. 60 and 300 min for photo-Fenton and TiO_2 photocatalysis, respectively, which indicates that the process is around 5 times quicker when iron is used. This is consistent with results
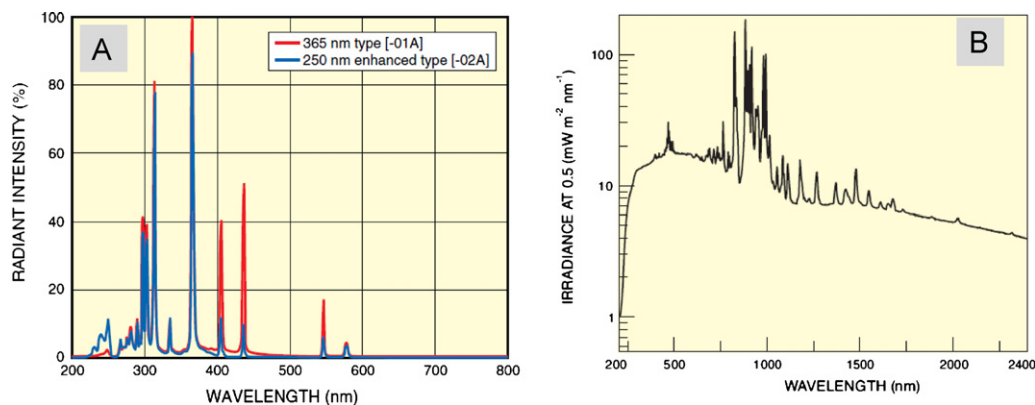

Fig. 2. (A) Radiant spectral distribution of UV spot light from Hamamatsu (365 nm-type red trace) and (B) spectral output of 150 W solar simulator (Oriel Model 6255) as provided by the suppliers [17,18].
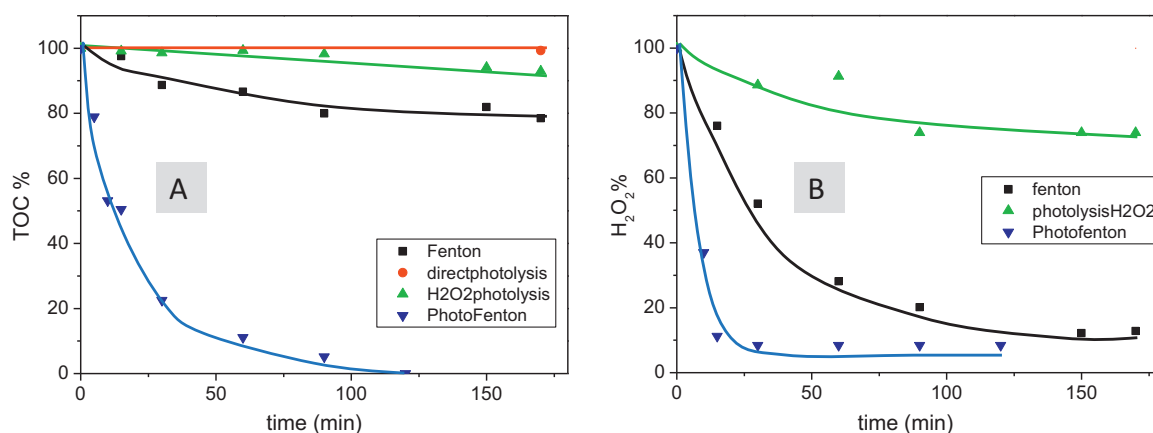
Fig. 3. Evolution of total organic carbon, TOC, (A) and H_2O_2 (B) as a function of time under different conditions using 40 ppm solutions of 3-chloropyridine in Milli-Q water. Direct photolysis (neither iron nor H_2O_2), H_2O_2 photolysis (presence of H_2O_2 but absence of iron), Fenton (iron, H_2O_2 in the dark), photo-Fenton (light + iron + H_2O_2). The 20 mL reactor and solar simulator (see text) was used in irradiation studies. When applicable, 0.88 mM $FeSO_4 \cdot 7H_2O$, $[H_2O_2]/[Fe^{2+}] = 10$.

found by Malato et al. for other pesticides considered as EU priority substances [19,20]. The authors concluded that photo-Fenton treatment is more appropriate than TiO_2 for treatment of those pesticides or mixtures of them. Only dimethoate was found to exhibit a mineralization rate quite similar in both photocatalytic treatments whereas in the other cases shorter times (ca. 4–5) were required when photo-Fenton was used.

In a previous study using the same experimental setup as in the present manuscript [21], selective photocatalytic oxidation of crotyl alcohol to crotonaldehyde was studied. It was found that the optimum TiO_2 concentration was ca. 6.7 g/L. Higher concentrations did not lead to better results probably because of the screening effect of excess particles which masks part of the photosensitive surface [22]. As TiO_2 concentration used in the present study (700 mg/L) was below that value, the possibility of excessive catalyst content accounting for the worse catalytic performance of TiO_2 as compared to photo-Fenton process can be ruled out.

Finally, differences in mineralization rates of UV photo-Fenton and solar photo-Fenton could be partly ascribed to the higher intensity of this lamp as compared to the solar simulator (618 and 360 mW cm^{-2}, respectively at 365 nm).
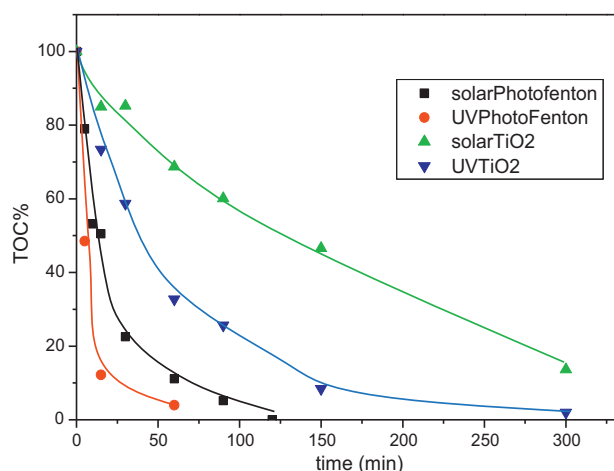

Fig. 4. Evolution of total organic carbon as a function of time, under different conditions, using 40 ppm solutions of 3-chloropyridine in Milli-Q water for reactions performed in the 20 mL reactor. Photo-Fenton studies: 0.88 mM $FeSO_4 \cdot 7H_2O$, $[[H_2O_2]/[Fe^{2+}] = 10$. TiO_2 photocatalysis: 700 mg/L TiO_2.
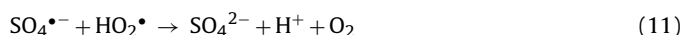
Given the faster degradation rates found for photo-Fenton process as compared to TiO_2 photocatalysis, subsequent experiments were performed using photo-Fenton methodology and solar light.

3.3. Influence of the presence of other inorganic ions in the medium

The presence of certain inorganic ions in the reaction medium has a significant inhibitory effect on the kinetics of degradation of pollutants by photo-Fenton process. These ions (phosphate, sulfate, fluoride, bromide, chloride...) can be part of the waters or be generated during the degradation of organic compounds (in our case, chloride during 3-chloropyridine degradation). The negative influence of these species may be due to the formation of certain less-active iron complexes, the reaction with hydroxyl radicals present to give rise to other less reactive radicals or the precipitation of iron ions. However, the negative effect on the kinetics of the reaction depends on the concentration of these ions in solution. Different authors have studied the influence of these species on the rate of degradation of organic pollutants at different concentration intervals [23–26]. On the other hand, some other ions, such as nitrate and perchlorate do not have a significant inhibitory effect on the photocatalytic mineralization process [27].

In the present study, the influence of chloride, sulfate and phosphate ions is considered.

The presence of chloride and/or sulfate ions may affect the mechanism of photo-Fenton in two different ways: (i) formation of ferric chloride and sulfate complexes that alter the distribution and reactivity of iron species ($FeCl^+$, $FeCl^{2+}$, $FeCl_2^+$, $FeSO_4^+$, $Fe(SO_4)_2^-$); (ii) neutralization of hydroxyl radicals and formation of some less reactive inorganic radicals ($Cl_2^{\bullet-}$, $Cl^\bullet$, $SO_4^{\bullet-}$) according to reactions 9–14. It is important to note that this effect is more significant for Cl^- ions. However, these radicals can contribute to some extent to the degradation of organic pollutants, since its oxidation potential is also high (E_0 ($Cl^\bullet/Cl^-$) = 2.41 V; $E_0(Cl_2^{\bullet-}/2Cl^-)$ = 2.09 V [6]).

$$HSO_4^- + OH^\bullet \rightarrow SO_4^{\bullet-} + H_2O \tag{9}$$

$$SO_4^{\bullet-} + H_2O_2 \rightarrow SO_4^{2-} + H^+ + HO_2^\bullet \tag{10}$$

$$SO_4^{\bullet-} + HO_2^\bullet \rightarrow SO_4^{2-} + H^+ + O_2 \tag{11}$$

$$Cl^- + {}^\bullet OH \rightarrow ClOH^{\bullet-} \tag{12}$$

$$ClOH^{\bullet-} + H^+ \rightarrow Cl^\bullet + H_2O \tag{13}$$

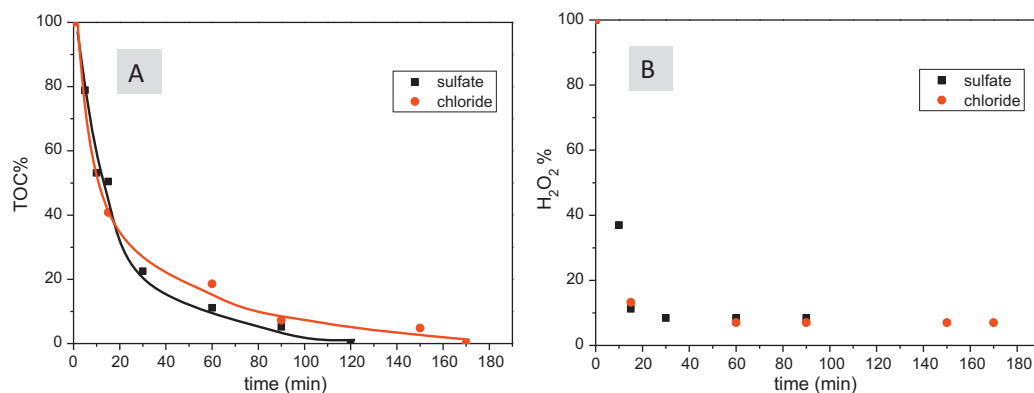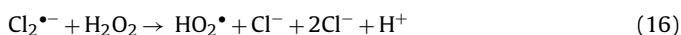$$Cl^\bullet + Cl^- \rightarrow Cl_2^{\bullet-} \tag{14}$$

Fig. 5. Photo-Fenton studies using the 20 mL reactor and the solar simulator as the irradiation source. (A) Evolution of total organic carbon (TOC) as a function of irradiation time from 40 ppm solutions of 3-chloropyridine in Milli-Q water. 0.88 mM Fe(II) using sulfate or chloride as the precursor, $[[H_2O_2]/[Fe^{2+}] = 10$. (B) Evolution of H_2O_2 as a function of irradiation time.

The radicals formed from Cl^- ions can also react with H_2O_2 (reactions (15)–(16)) producing less active radicals and increasing the global consumption of this reagent.

$$Cl^\bullet + H_2O_2 \rightarrow HO_2^\bullet + Cl^- + H^+ \tag{15}$$

$$Cl_2^{\bullet-} + H_2O_2 \rightarrow HO_2^\bullet + Cl^- + 2Cl^- + H^+ \tag{16}$$

As regards the influence of the presence of phosphates on ferric ions, very insoluble complexes can be formed at neutral or acidic pH ($FePO_4 \cdot 2H_2O$), thus removing dissolved iron from the medium and therefore preventing the catalytic process. In fact, the precipitation of ferric phosphate is a widely used method to remove iron from solution [28,29]. The formation of these precipitates takes place in a wide pH range and is independent of temperature operation, being more favorable at a pH between 3.5 and 4. Since these complexes are soluble only in strongly acidic pH (<1.5), the Fenton process (pH 2.8) should be conducted in the absence of phosphate ions.

In order to study the effect of chloride and sulfate species, two different iron (II) precursors (ferrous sulfate and chloride) were compared (Fig. 5). Initial pH adjustment to 2.8 was carried out with 0.5 M H_2SO_4 or HCl, respectively.

As commented above, the presence of chloride and sulfate ions can adversely affect the photo-Fenton process in two different ways: (1) by altering the distribution and reactivity of iron species through formation of diverse iron complexes and (2) through neutralization of hydroxyl radicals and formation of some other less oxidant inorganic radicals. Furthermore, radicals formed from chloride ions can also react with H_2O_2. Given the fact that photo-Fenton experiments were conducted with no additional supply of H_2O_2 as

the reaction proceeded, the different influence of inorganic ions becomes more evident for longer irradiation times when hydrogen peroxide and thus hydroxyl radicals are scarce. This could explain the fact that even though TOC% evolution is quite similar for ferrous sulfate and chloride during the first 20 min of irradiation, complete mineralization of 3-chloropyridine requires 120 min and 170 min, respectively (Fig. 5A). This also justifies the choice of ferrous sulfate as the iron precursor.

A study on the influence of phosphate ions at two different concentrations (2 mg/L and 1 g/L) was also conducted. The lowest limit correspond to the total phosphorus requirement for discharges from urban waste water treatment plants to sensitive areas which are subject to eutrophication (Council Directive of 21-5-91 concerning urban waste water treatment, Official Journal of the European Communities No L 135/49 of 30.5.91). The highest value is intended to clearly evidence the ability of phosphate ions to remove dissolved iron. Therefore, as shown in Fig. 6 a phosphate concentration as low as 2 mg/L can already slow down mineralization of 3-chloropyridine, whereas 1 g/L has a dramatic effect on reaction rate. In fact, at this concentration, a few minutes after the reaction mixture has been exposed to light, solution became cloudy, leading to a yellowish-white precipitate of ferric phosphate. The precipitation of iron also accounts for the slow decomposition of H_2O_2 in the presence of 1 g/L phosphate (Fig. 6B).

All the above-mentioned experiments were performed in Milli-Q water. At this point it was decided to use tap water in order to operate under "more real" conditions and check the possible influence of dissolved ions in 3-chloropyridine mineralization. Water management in Cordoba (Spain) corresponds to a public limited
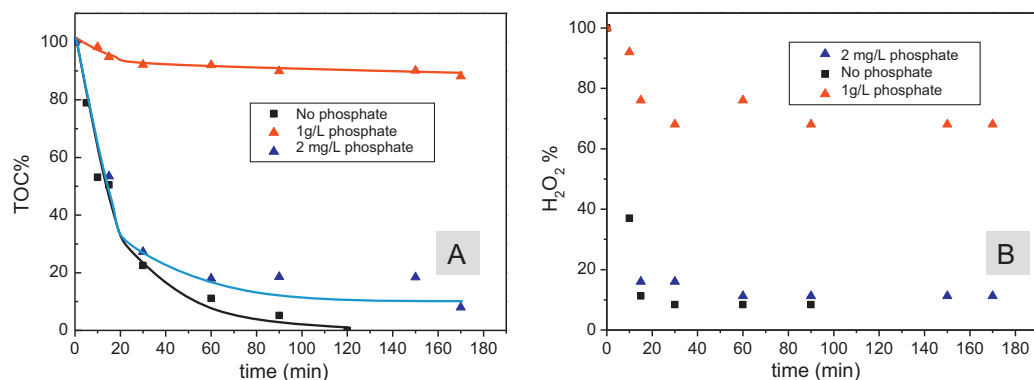

Fig. 6. Photo-Fenton studies using the 20 mL reactor and the solar simulator as the irradiation source and different concentrations of phosphate. (A) Evolution of total organic carbon (TOC) as a function of irradiation time from 40 ppm solutions of 3-chloropyridine in Milli-Q water. 0.88 mM $FeSO_4 \cdot 7H_2O$, $[[H_2O_2]/[Fe^{2+}] = 10$. (B) Evolution of H_2O_2 as a function of time.
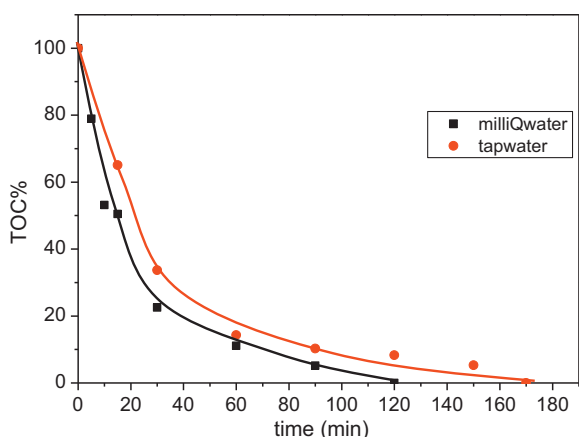
Fig. 7. Photo-Fenton studies using the 20 mL reactor and the solar simulator as the irradiation source. Evolution of total organic carbon (TOC) as a function of irradiation time from 40 ppm solutions of 3-chloropyridine in Milli-Q and tap water. 0.88 mM $FeSO_4 \cdot 7H_2O$, $[[H_2O_2]/[Fe^{2+}] = 10$.
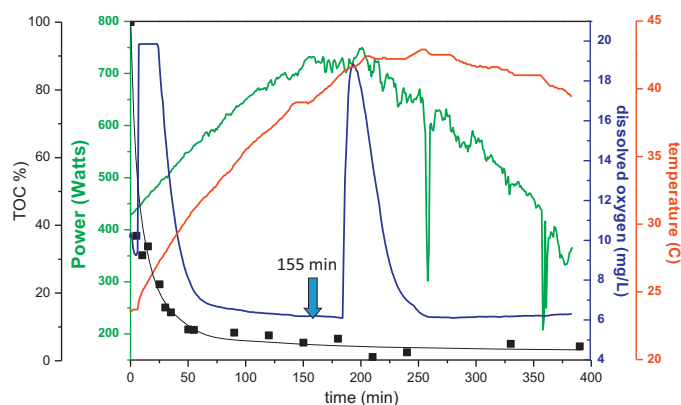

Fig. 8. Photo-Fenton degradation of 30 L of a 40 ppm solution of 3-chloropyridine in tap water, using the solar pilot plant. 0.88 mM iron (II) sulfate, $[H_2O_2]/[Fe^{2+}] = 10$. The vertical arrow indicates the moment when 5.5 MJ sun energy had reached the reactor and, according to the extrapolation of results at lab scale using the solar simulator, total mineralization should have been achieved.
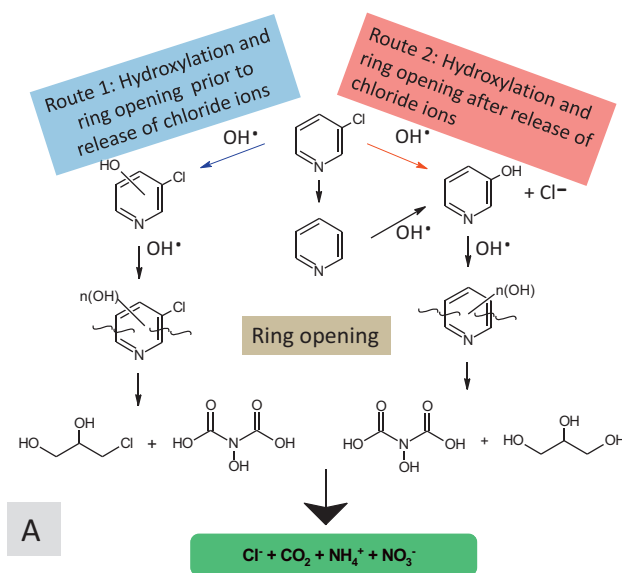
company called EMACSA. According to their own analyses, tap water supplied had a conductivity of ca. 280 μS/cm and a moderate content in $CaCO_3$ and HCO_3^- (ca. 100 mg/L each). Fig. 7A compares mineralization of a 40 ppm 3-chloropyridine solution using Milli-Q and tap water. As can be seen, mineralization is slightly slower in the latter case probably as a result of the presence of some dissolved ions. In fact, carbonate and bicarbonate ions are known to have a negative effect on Fenton process as hydroxyl radical scavengers thus leading to carbonate radicals which are particularly ineffective for degradation of organic matter [30]. In any case, under our experimental conditions there is full mineralization after 170 min of irradiation.

3.4. Scaling-up of the photo-Fenton process: from 20 mL to 30 L

The next step was to verify if results obtained at lab scale could be extrapolated to the pilot plant. As explained above, under our experimental conditions, an experiment from a 40 ppm solution of 3-chloropyridine (in tap water) required 170 min of irradiation of the solar simulator for complete mineralization. An integration of the lamp power over the time led to a total energy requirement of 3672 J. Therefore, for 30 L of a 40 ppm solution of 3-chloropyridine, energy required would be $3672 \times 1500 = 5.5$ MJ (scaling factor of 1500 from 20 mL to 30 L). This is consistent with the results found for experiments in the pilot plant (Fig. 8). The vertical arrow indicates the moment when 5.5 MJ had reached the reactor and, as evidenced by TOC evolution, mineralization had been completed. In order to make sure of that, some extra 15 mL H_2O_2 (ca. half the initial amount) were added thus resulting in a sharp rise in dissolved oxygen signal whereas TOC remained below 5% (probably the experimental error at these trace levels). Finally, the lower dissolved oxygen value at the end of the experiment as compared to the beginning is just a result of the increase in temperature [31]. Therefore, at the end of the experiment the value was 6.3 mg/L which is ca. the 100% saturation value at 39.4 °C.

3.5. Toxicity studies

As commented in the introduction, photocatalysis can be used to degrade toxic pollutants as a previous step, coupled to a subsequent
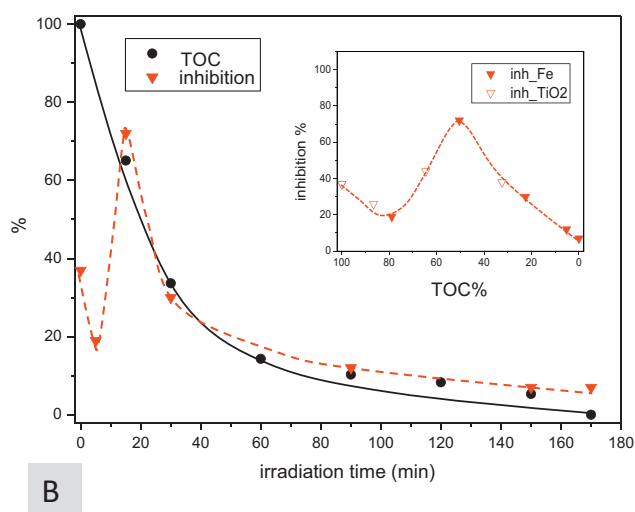

Fig. 9. (A) Degradation pathway proposed in a previous work [14]. (B) Results found for Photo-Fenton process using the 20 mL reactor and the solar simulator as the irradiation source expressed as total organic carbon (TOC) or inhibition (*V. fischeri*, 15 min assays) as a function of irradiation time. Reaction conditions: 40 ppm solution of 3-chloropyridine in tap water. 0.88 mM iron (II) sulfate, $[[H_2O_2]/[Fe^{2+}] = 10$. The inset includes results for TiO_2 photocatalysis (700 mg/L Degussa P25).

biological treatment. Liu et al. [32] tried to correlate the structure of pyridine and pyridine derivatives with their biodegradability by estuarine sediment microorganisms under anaerobic conditions as well as their toxicity (*V. fischeri* assay). Their results showed that 3-hydroxypyridine (one of the first metabolites in the proposed photocatalytic degradation pathway [14], Fig. 9A) is more susceptible to biotransformation than 3-chloropyridine or pyridine. Moreover, 15-min EC_{50} values (*V. fischeri*) for 3-chloropyridine, pyridine and 3-hydroxypyridine were 0.91, 4.73, and 6.25 mmol/L respectively, thus evidencing that 3-hydroxypiridine is about 7 times less toxic than 3-chloropyridine.

Nevertheless, it is possible that as photocatalytic degradation proceeds, some intermediates more toxic than 3-chloropyridine are formed. In order to cast further light on that, toxicity (*V. fischeri* assay) was studied as a function of irradiation time. Results for solar photo-Fenton are represented in Fig. 9B. As can be seen, there is an initial decrease in toxicity (which would be consistent with the above-mentioned lower toxicity of hydroxypyridines as compared to chloropyridines followed by an increase in toxicity with a maximum at ca. 15 min (72% inhibition, 50% TOC) after which toxicity continuously drops to a final value of ca. 7% for total organic carbon disappearance. In the case of TiO_2 photocatalysis there is 38% inhibition after 210 min irradiation which is consistent with the much slower degradation rate (ca. 32% TOC remaining for that time, see Fig. 4). More interestingly, if we compare inhibition percentages obtained for TiO_2 photocatalysis and photo-Fenton process at the same TOC value, results seem to follow a similar trend (see inset of Fig. 9B) which could suggest similar degradation mechanisms.

4. Conclusions

A comparative study of photocatalytic degradation of 3-chloropyridine as a model compound of pyridine pesticides has been carried out both in the homogeneous (photo-Fenton) and heterogeneous (TiO_2) phase using UV and solar light. Results showed that photo-Fenton process is more efficient than TiO_2 photocatalysis (ca. 5 times faster) though complete mineralization could be achieved by both technologies. Moreover, under our experimental conditions no mineralization was obtained by direct photolysis whereas the addition of H_2O_2 led to a 7% mineralization after 3 h of solar irradiation.

Iron (II) sulfate is preferable to iron (II) chloride as the metal precursor in photo-Fenton process and the presence of phosphate in wastewaters is quite critical and should be avoided since it results in iron (III) precipitation and affects the mineralization process even at low concentrations (2 mg/L).

Results found at lab scale (20 mL, solar simulator) where successfully extrapolated at larger scale (30 L, sun light) thus confirming the validity of photo-Fenton to degrade water polluted with this type of chemical. Toxicity studies (*V. fischeri*) evidenced that some chemicals more toxic that 3-chloropyridine itself are formed as the reaction proceeds.

References

[1] A.T. Shawaqfeh, F.A. Al Momani, Solar Energy 84 (2010) 1157–1165.
[2] C. Mendoza-Marin, P. Osorio, N. Benitez, Journal of Hazardous Materials 177 (2010) 851–855.
[3] U.I. Gaya, A.H. Abdullah, Journal of Photochemistry and Photobiology C 9 (2008) 1–12.
[4] E.M.R. Rocha, V.J.P. Vilar, A. Fonseca, I. Saraiva, R.A.R. Boaventura, Solar Energy 85 (2011) 46–56.
[5] M.E.T. Sillanpaa, T.A. Kurniawan, W.H. Lo, Chemosphere 83 (2011) 1443–1460.
[6] C. Sirtori, A. Zapata, I. Oller, W. Gernjak, A. Aguera, S. Malato, Water Research 43 (2009) 661–668.
[7] S. Malato, J. Blanco, M.I. Maldonado, I. Oller, W. Gernjak, L. Perez-Estrada, Journal of Hazardous Materials 146 (2007) 440–446.
[8] I. Oller, S. Malato, J.A. Sanchez-Perez, Science of the Total Environment 409 (2011) 4141–4166.
[9] S. Malato, J. Blanco, A. Vidal, C. Richter, Applied Catalysis B 37 (2002) 1–15.
[10] A.M. Amat, A. Arques, M.A. Miranda, S. Segui, Solar Energy 77 (2004) 559–566.
[11] J.C. Colmenares, M.A. Aramendia, A. Marinas, J.M. Marinas, F.J. Urbano, Journal of Molecular Catalysis A 331 (2010) 58–63.
[12] D.R. Stapleton, D. Mantzavinos, M. Papadaki, Journal of Hazardous Materials 146 (2007) 640–645.
[13] D.R. Stapleton, I.K. Konstantinou, D. Mantzavinos, D. Hela, M. Papadaki, Applied Catalysis B 95 (2010) 100–109.
[14] M.A. Aramendia, J.C. Colmenares, S. Lopez-Fernandez, A. Marinas, J.M. Marinas, J.M. Moreno, F.J. Urbano, Catalysis Today 138 (2008) 110–116.
[15] B.F. Abramovic, V.B. Anderluh, A.S. Topalov, F.F. Gaal, Applied Catalysis B 48 (2004) 213–221.
[16] G. Kyriacou, K. Tzoanas, I. Poulios, Journal of Environment Science and Health, Part A: Environmental Science 32 (1997) 963–977.
[17] http://sales.hamamatsu.com/assets/pdf/parts_L/LC8_TLSZ1008E02.pdf, (accessible at 17.08.12).
[18] http://search.newport.com/?x2=sku&q2=6255, (accessible at 17.08.12).
[19] M.I. Maldonado, P.C. Passarinho, I. Oller, W. Gernjak, P. Fernandez, J. Blanco, S. Malato, Journal of Photochemistry and Photobiology A 185 (2007) 354–363.
[20] I. Oller, W. Gernjak, M.I. Maldonado, L.A. Perez-Estrada, J.A. Sanchez-Perez, S. Malato, Journal of Hazardous Materials 138 (2006) 507–517.
[21] F.J. López-Tenllado, A. Marinas, F.J. Urbano, J.C. Colmenares, M.C. Hidalgo, J.M. Marinas, J.M. Moreno, Applied Catalysis B (2012), http://dx.doi.org/10.1016/j.apcatb.2012.02.015, in press.
[22] J.M. Herrmann, Catalysis Today 53 (1999) 115–129.
[23] J. Soler, A. Garcia-Ripoll, N. Hayek, P. Miro, R. Vicente, A. Arques, A.M. Amat, Water Research 43 (2009) 4441–4450.
[24] L.G. Devi, K.S.A. Raju, S.G. Kumar, K.E. Rajashekhar, Journal of the Taiwan Institute of Chemical Engineering 42 (2011) 341–349.
[25] M. Jimenez, I. Oller, M.I. Maldonado, S. Malato, A. Hernandez-Ramirez, A. Zapata, J.M. Peralta-Hernandez, Catalysis Today 161 (2011) 214–220.
[26] C. Sirtori, A. Zapata, W. Gernjak, S. Malato, A. Lopez, A. Aguera, Water Research 45 (2011) 1736–1744.
[27] J. De Laat, G.T. Le, B. Legube, Chemosphere 55 (2004) 715–723.
[28] E. Neyens, J. Baeyens, Journal of Hazardous Materials 98 (2003) 33–50.
[29] J.J. Pignatello, E. Oliveros, A. MacKay, Critical Reviews in Environment Science and Technology 36 (2006) 1–84.
[30] W. Gernjak. Doctoral Thesis, University of Natural Resources and Applied Life Sciences, Vienna Austria, 2006.
[31] http://water.epa.gov/type/rsl/monitoring/vms52.cfm
[32] S.M. Liu, C.H. Wu, H.J. Huang, Chemosphere 36 (1998) 2345–2357.